

# Accuracy of TRMM precipitation data in the southwest monsoon region of China

Zhu Guofeng<sup>1,2</sup> · Qin Dahe<sup>2</sup> · Liu Yuanfeng<sup>1</sup> · Chen Fenli<sup>1</sup> · Hu Pengfei<sup>1</sup> ·  
Chen Dongdong<sup>1</sup> · Wang Kai<sup>1</sup>

Received: 25 September 2014 / Accepted: 19 March 2016 / Published online: 1 April 2016  
© Springer-Verlag Wien 2016

**Abstract** Accurate, high-resolution precipitation data is important for hydrological applications and water resource management, particularly within mountainous areas about which data is presently scarce. The goal of this study was to assess the accuracy of TRMM 3B43 precipitation data from the southwest monsoon region of China between 1998 and 2011 based on the correlation coefficients, regression, and geostatistical methods. We found a strong correlation between TRMM 3B43 data and observational data obtained from meteorological stations, but the TRMM 3B43 precipitation data was consistently lower than that obtained from the weather stations. The TRMM 3B43 data was significantly different from the data obtained by weather stations located in the northwest and northeast regions of the Hengduan Mountains. The spatial distribution of precipitation obtained from TRMM 3B43 was also different from meteorological data, but the deviation was predominantly distributed along the northern longitude and southern latitude. In addition, the TRMM data more accurately reflected the regional precipitation patterns. Our results indicate that the TRMM 3B43 data should be used for hydrological applications and water resource management at meteorological stations that have a sparse and uneven distribution of observation stations in the southwest monsoon region.

Accuracy of TRMM precipitation data in the southwest monsoon region of China

## 1 Introduction

Precipitation is a complex, natural phenomenon characterized by significant temporal and spatial variability. It is a major component of the hydrological cycle and has a significant influence on hydrology, climatology, ecology, and agricultural development (Abbott et al. 1986; Yair and Raz. 2004; Liu and Fu. 2007; Baguis et al., 2010; Liu et al. 2011; Zhu et al. 2012).

According to the World Meteorological Organization (WMO) standards, the meteorological station distribution density should be denser in mountainous areas than in the plains (WMO 1992). However, the meteorological station distribution in the western mountainous region of China is much sparser than it is in the plains. There are 752 main meteorological stations located in China, of which 121 are located in the southwest monsoon region. Rain gauge measurements cannot provide adequate and reliable precipitation data due to the spatial limitations of point-based measurements and the relatively sparse distribution of observation stations (Javanmard et al. 2010). Remote sensing has the potential to overcome the limitations of large-scale spatial variations (Olson et al. 1996; Kummerow et al. 1998a, b; Iguchi et al. 2000; Su et al. 2008).

Since the launch of The Tropical Rainfall Measuring Mission (TRMM) with high-resolution space-borne microwave imaging instrument (TMI) in 1997 (Simpson et al. 1988; Olson et al. 1996; Awaka et al. 1998; Kummerow et al. 1998a; Fu and Liu. 2003; Schumacher and Houze 2006; Yamamoto et al. 2008; Liu et al. 2010; Yu et al. 2010; Zeng and Li 2011), several studies regarding the prospecting of rainfall data using remote sensing have been reported.

✉ Zhu Guofeng  
guofengzhu@me.com

<sup>1</sup> College of Geography and Environment Science of Northwest Normal University, Lanzhou 730070, China

<sup>2</sup> State Key Laboratory of Cryosphere Sciences, Cold and Arid Region Environmental and Engineering Research Institute, Chinese Academy of Sciences, Lanzhou 730000, China

TRMM precipitation data has been widely evaluated and has shown better performance with many applications (Dinku et al. 2007), including hydrological modeling (Li et al. 2012; Su et al. 2008; Swenson and Wahr 2009), flood prediction (Li et al. 2009), rainfall erosivity estimation (Vrieling et al. 2010), and climatological studies (Islam and Uyeda 2007). Moreover, multiple studies have discussed the high variability of precipitation at small scales (Krajewski et al. 2003).

The TRMM, an American-Japanese earth satellite observation mission, was launched in 1997 (to an altitude of 350 km) in order to provide a better understanding of the precipitation structure and heating patterns of the earth's tropical regions (Zheng and Bastiaanssen 2013). Operating in non-sun-synchronous orbits, the satellite has an orbital period of 91 min, making 16 orbits per day, thereby providing good coverage of the tropics. TRMM's onboard instruments include the precipitation radar (PR), microwave imager (TMI), visible and infrared scanner (VIRS), Cloud and Earth's Radiant Energy System, and Lightning Imaging Sensor. The most prominent is the PR. At its launching stage, the TRMM PR was the first space-borne radar that was designed to capture a more comprehensive structure of rainfall than any previous space-borne sensor. This instrument has been producing three-dimensional spatial rainfall data unprecedented by any previous scientific spacecraft.

Based on the precipitation data obtained from the TRMM and weather observation stations, the spatial and temporal variability of precipitation in the China southwest monsoon region of China was studied using the Kriging interpolation method. The primary objective of the study was to obtain the most accurate precipitation estimate resolution for hydrological, ecology, meteorology, and climatology studies. The specific objectives include (a) to document seasonal variations in the spatial distribution between the TRMM 3B43 data and weather observation data in the southwest monsoon region and (b) to study the spatial distribution and temporal variation of precipitation in the Southwest monsoon region.

## 2 Study area, data and methods

### 2.1 Study area

The China southwest monsoon region lie in the southeast of Tibet plateau, most area of Yunnan province, and the southwest of Sichuan (21° 10'–34° 00' N; 92° 20'–104° 30' E), with an area of 1,100,000 km<sup>2</sup> (Fig. 1), consisting of a series of mountain ranges and rivers (Li and Su 1996), including Mt. Min, Mijing River, Mt. Qionglai, Daduhe River, Mt. Daxue, Yalongjiang River, Mt. Shaluli, Mt. Habaxue, Mt. Yulong, Jinshajiang River, Mt. Ningjing, Mt. Yunling, Lancangjiang River, Mt. Taniantawen, Mt. Tanggula, Mt. Ailao Nujiang River, and Mt. Boshulalin, and Mt. Gaoligong, Mt. Gongga.

This region has the highest peak (7556 m) and is located in the central area of the China southwest monsoon region. The mountainous areas above 5000 m accounted for 25 % of the southwest monsoon region. The China southwest monsoon region is also a world famous longitudinal range-gorge region which was characterized by north-south rivers and aligned from west to east (You et al. 2005; Zeng and Li 2011; Zhu et al. 2012). It is obstruction for the eastern Asia monsoon forward to meet the southern Asia monsoon. The topography becomes lower from northwest to southeast. Located in the subtropical and plateau temperate climate zones, the climate is vertically variable due to the complex mountainous topography. The soil and biodiversity are remarkable because of the monsoonal climate and the large vertical gradient. This typical monsoonal climate region was controlled by the South Asia monsoon as well as the East Asia monsoon. In addition, it was also influenced by the Qinghai-Tibet plateau monsoon and westerlies. Correspondingly, moisture transfer has the obvious seasonal change. In winter and spring, the moisture was mainly from the westerlies. In summer, moist maritime air originated from the Bay of Bengal and the South China Sea. In autumn, it was mainly obtained from the western Pacific Ocean. Monsoonal circulation expanded to 40° N in the beginning of August, but retreated to 30° N in October in the southwest monsoon region. Monsoon strengthens or weakens; advances or retreats, often results in floods or droughts. The winter monsoon period is from December to April. The summer monsoon period is from May to October, with precipitation accounting for about 90 % of the annual total precipitation (Li and Su 1996). Owing to the topography, the abundant precipitation was in the accumulation area and the low temperature in the high altitude area.

### 2.2 Data and methods

#### 2.2.1 Data

The TRMM 3B43 data (1998–2011) was obtained from NASA (<http://www.nasa.gov/topics/earth>) at a spatial resolution of 0.25° × 0.25°. Data from 46 meteorological stations in the monsoon region of Southwest China was obtained from the Meteorology Center and the National Meteorological Administration of the PR China (<http://www.nmic.gov.cn>) (Fig. 1, Table 1). Forty-six national weather station data in the southwest monsoon region were selected using the RClimDex and RHtest (<http://cccma.seos.uvic.ca/ETCCDI/software.shtml>) (Fig. 1, Table 1). The TRMM data and weather observation data were analyzed in the specific time periods of spring, summer, autumn, and winter, respectively. Spring was defined as the time period between March and May; summer was between June and August; autumn was designated as the period between September and November;

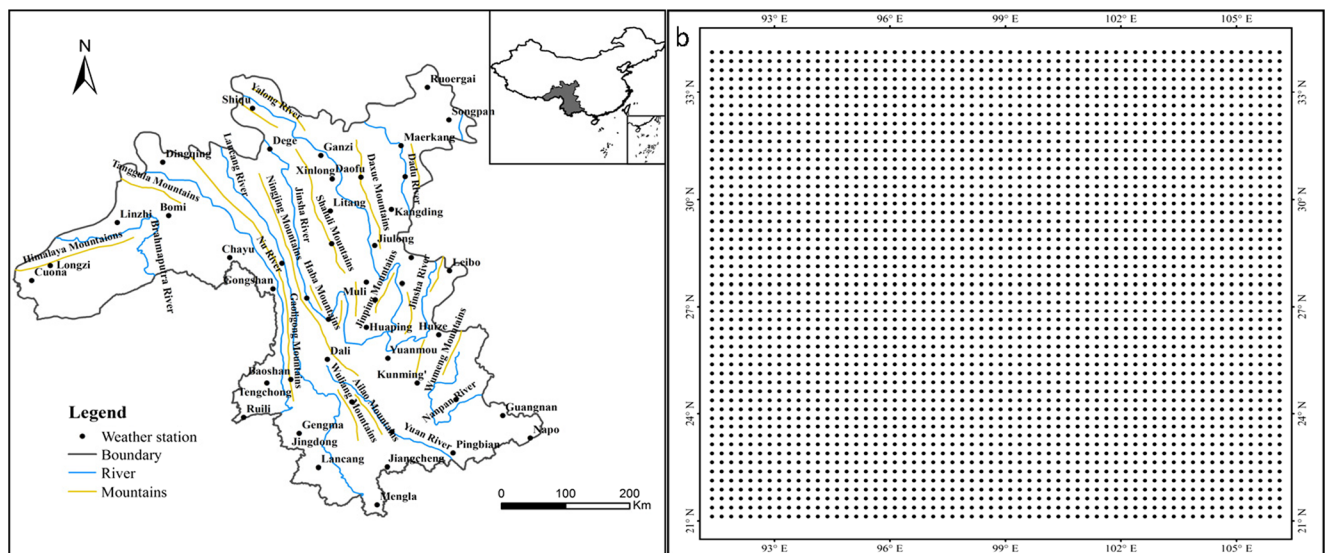


**Fig. 1** Location of the southwest China monsoon region and the TRMM grid. **a** Distribution of 46 meteorological stations, which were built between 1952 and 1960, and from which the complete and continuous data after 1960 has been obtained. **b** Distribution of the TRMM grid. TRMM provides precipitation information using several space-borne

instruments to increase our understanding of the interactions between water vapor, clouds, and precipitation. The TRMM 3B43 data was obtained from NASA (<http://www.nasa.gov/topics/earth>) at a spatial resolution of  $0.25^{\circ} \times 0.25^{\circ}$

**Table 1** Characteristics of the meteorological stations in southwest China monsoon region

Station	Longitude (°)	Latitude (°)	Altitude (m)	Station	Longitude (°)	Latitude (°)	Altitude (m)
Baoshan	99.18	25.12	1652.2	Leibo	103.58	28.27	1255.8
Barkam	102.14	31.54	2664.4	Lijiang	100.13	26.52	2392.4
Bomi	95.77	29.87	2736	Linzhi	94.03	29.07	2991.8
Chayu	97.47	28.65	2327.6	Litang	100.16	30.00	3948.9
Cuona	91.95	27.98	4280.3	Longzi	92.47	28.42	3860
Dali	100.11	25.42	1990.5	Luxi	103.77	24.53	1704.3
Daocheng	100.18	29.03	3528	Mengla	101.57	21.48	631.9
Daofu	101.07	30.59	2957.2	Muli	101.16	27.56	2426.5
Dege	98.35	31.48	3349	Napo	105.08	23.42	794.1
Deqin	98.55	28.29	3319	Pingbian	103.68	22.98	1414.1
Dingqing	95.36	31.25	3873.1	Ruili	97.85	24.02	776.6
Ganzi	100.00	31.37	3393.5	Shiqu	98.06	32.59	4518
Gengma	99.40	23.55	1104.9	Songpan	103.34	32.39	2850.7
Gongshan	98.40	27.45	1583.3	Tengchong	98.05	25.02	1654.6
Guangnan	105.07	24.07	1249.6	Xianggeli	99.70	27.49	3281
Huaping	101.16	26.38	1244.8	Xiaojing	102.21	31.00	2369.2
Huize	103.28	26.42	2110.5	Xichang	102.16	27.54	1590.9
Jiangchang	101.85	22.58	1120.5	Xinlong	100.19	30.56	3890
Jingdong	100.87	24.47	1162.3	Yanyuan	101.31	27.26	2545
Jiulong	101.30	29.00	3009	Yuanjiang	101.98	23.60	400.9
Kangding	101.58	30.03	2615.7	Yuanmou	101.87	25.73	1120.6
Kunming	102.65	25.42	1886.5	Yuexi	102.31	28.39	1659.5
Lancang	99.93	22.57	1054.8	Zoige	102.58	33.35	3439.6

Meteorological stations were built between 1952 and 1960, and the complete and continuous data after 1960 have been obtained

and winter was defined as the time between December and February of the subsequent year.

### 2.2.2 Methods

The Chinese southwest monsoon region is a stereotypical mountainous region (You et al., 2005), whose mountains divide the areas according to east and west as well as by north and south. The climate in this region is influenced by the spatial distribution of the southwest monsoons and westerly winds. The TRMM data is usually validated for oceanic or plains regions, but few have been verified in the mountainous areas. The objective of the present study is to validate the TRMM 3B43 data in the China southwest monsoon region using correlation analysis, regression analysis, and geostatistical methodologies. Geostatistical analysis is utilized as the main tool for analyzing precipitation data (Nyberg 1996; Crave and Gascuel-Odux 1997; Ba'rdossy and Lehmann 1998; Western et al. 1998, 1999). Using Kriging interpolation (Goovaerts 1997; Yamamoto 2005, 2007), correlation analysis was also used to discuss the dominant factors leading to underestimation of precipitation.

## 3 Results and discussion

### 3.1 Difference of TRMM 3B43 and weather station precipitation data

The meteorological observation data obtained from different seasons was closely correlated to the TRMM 3B43 precipitation data (Table 2); the correlation indices in Longzi, Gongshan, and Ruili stations were 0.478 ( $P < 0.01$ ), 0.674 ( $P < 0.01$ ), and 0.688 ( $P < 0.01$ ), respectively. The correlation was relatively weak, and other stations were also significantly correlated ( $R > 7.5$ ,  $P < 0.01$ ), indicating that the distribution and variation trends of the TRMM 3B43 precipitation data were consistent with that of the meteorological observation data. The determination coefficient of the TRMM 3B43 data and observational data is  $R^2 = 0.867$ ,  $K = 0.662$  (Fig. 2). Overall, the TRMM 3B43 precipitation data was much lower overall than the observed data. The variation trend of the TRMM 3B43 data was approximately consistent with meteorological observation data. Of interest, the observed data is point data while TRMM provides grid data; thus, the correlation analysis may conceal differences between the single point data and corresponding TRMM 3B43 grid data, which means that the precipitation may be influenced by terrain, elevation, and atmospheric circulation. With the spatial and temporal discontinuity and nonlinearity of the data distribution, the regression analysis was used in this study to understand the relationship between weather station and TRMM 3B43 data. The regression slope  $K$  of meteorological station data and

**Table 2** The correlation coefficient between TRMM 3B43 precipitation data and meteorological station precipitation data

Station	Spring	Summer	Autumn	Winter	Year
Daocheng	0.854**	0.929**	0.971**	0.932**	0.984**
Daofu	0.883**	0.869**	0.917**	0.544**	0.959**
Dege	0.892**	0.784**	0.934**	0.32	0.956**
Deqin	0.469**	0.692**	0.739**	0.928**	0.788**
Dingqing	0.861**	0.866**	0.932**	0.688**	0.964**
Ganzi	0.959**	0.868**	0.936**	0.896**	0.971**
Gongshan	0.578**	0.606**	0.696**	0.738**	0.674**
Huaping	0.929**	0.648**	0.892**	0.535**	0.923**
Jiulong	0.961**	0.837**	0.973**	0.564**	0.966**
Kangding	0.937**	0.884**	0.908**	0.955**	0.951**
Linzi	0.597**	0.827**	0.881**	0.670**	0.697**
Longzi	0.444**	0.690**	0.775**	0.036**	0.478**
Luxi	0.931**	0.868**	0.960**	0.674**	0.947**
Mengla	0.835**	0.918**	0.856**	0.951**	0.924**
Napo	0.841**	0.898**	0.965**	0.947**	0.903**
Pingbian	0.850**	0.644**	0.787**	0.940**	0.807**
Ruili	0.866**	0.577**	0.973**	0.954**	0.775**
Tengchong	0.829**	0.848**	0.945**	0.951**	0.901**

\*\* $P < 0.01$ ; \* $P < 0.05$

TRMM 3B43 data captures the difference between the TRMM 3B43 as well as the observed data (Fig. 2). The results indicate that the TRMM 3B43 data overestimate or underestimate the percentage (Eq. 1, Table 3).

$$B = (K - 1) \times 100\% \quad (1)$$

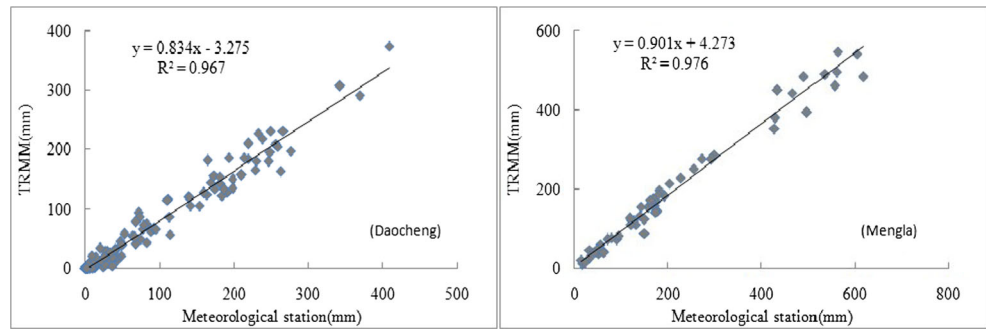
In Eq. 1,  $B$  represents the actual deviation; when the value is greater than 0, the TRMM 3B43 data represents an overestimate while a value less than 0 signifies an underestimation.  $K$  is represented in units of percent, while  $K$  represents the slope of regression equation.

### 3.2 Spatial distribution deviation of the TRMM 3B43 and meteorological data by season

The spatial distribution deviation of the TRMM 3B43 and observation data was obtained using the Kriging interpolation method (Fig. 3). The TRMM data in the southwest monsoon region underestimated the observed precipitation data by 22.9%. The deviation of the spatial distribution was greater in winter (Fig. 3; Table 3), and the deviation increased progressively from west to east in the northern southwest monsoon region and became smaller in the middle regions (lower than 25%). The high deviation value areas were distributed along the south of Wuliang Mt., and some areas were distributed in the northern parts of the southwest monsoon region,



**Fig. 2** Scatter plots of the TRMM 3B43 data against meteorological station precipitation data. Meteorological station precipitation data is on the x axis and TRMM 3B43 precipitation data is on the y axis



where in the precipitation, deviation was between 30 and 40 %. In different seasons, the deviation between TRMM 3B43 precipitation and observed data varied, but all were distributed along the longitudinal mountains in the northern areas and along the latitude in the southern regions. The deviations in spring, summer, autumn, and winter were 21.8, 22.2, 20.4, and 27.1 %, respectively. The deviation was the lowest during the spring and in other areas other than the southeast of the Tibetan Plateau and the southern region of Wuliang Mt. During the summer months (Fig. 3b), the deviation in spatial distribution was similar to the overall annual deviation, indicating that the precipitation in summer determined the overall trend of annual precipitation and its spatial distribution. The

deviation equivalent area was distributed along the longitudinal mountains in the northern region and along the southern latitude. The deviation was less in the central regions (less than 20 %). In the northeast, northwest, and southwest regions, the deviation was greater (greater than 30 %). In other areas, the deviation was between 20 and 30 %. In autumn (Fig. 3c), the deviation was between 20 and 40 % in the south of Mt. Hengduan. The deviation was highest in the northwest, northeast, and middle of Nu River, which was about 40 %. In winter (Fig. 3d), the deviation in the northern region of the southwest monsoon region was large, at about 40 %, but small in the southwest monsoon region, at roughly 20 %. As a whole, the TRMM 3B43 precipitation data was lower than

**Table 3** Mean deviation of TRMM 3B43 precipitation data and meteorological station precipitation data (Unit: %)

Station	Spring	Summer	Autumn	Winter	Year	Station	Spring	Summer	Autumn	Winter	Year
Baoshan	-26	-5	16	8	-1.71	Leibo	-17	-32	-11	-14	-18.61
Bomi	-41	-38	15	59	-1.28	Lijiang	-29	-29	-28	-58	-36.00
Chayu	-10	-77	-73	-48	-52.07	Linzi	-65	-17	-28	-78	-46.74
Cuona	-33	-106	-54	-28	-55.30	Longzi	-79	-42	-51	-99	-67.93
Dali	-14	-9	-20	-5	-12.00	Luxi	2	-16	8	11	1.38
Daofu	-44	-52	-53	-76	-56.25	Barkam	-32	-47	-36	-33	-37.00
Daocheng	-29	-18	-20	-29	-24.00	Mengla	-13	64	1	-21	7.69
Dege	-25	-41	-22	-80	-42.00	Muli	-29	-60	-51	-43	-45.75
Deqin	-79	-43	-66	-24	-53.00	Napo	43	15	3	-31	7.26
Dingqing	-28	-12	-17	-59	-29.00	Pingbian	-2	-27	6	7	-3.76
Ganzi	-24	-31	-29	-36	-30.00	Ruili	-4	-33	13	12	-3.13
Gengma	5	11	14	-3	6.91	Zoige	-44	-37	-40	-55	-44.00
Gongshan	-45	-64	-57	95	-17.75	Shiqu	-39	-32	-32	-25	-32.00
Guangnan	2	17	-14	-6	-0.38	Songpan	-29	-67	-42	-31	-42.25
Huaping	-31	-12	-19	-54	-29.00	Tengchong	-25	10	9	9	0.57
Huize	-9	-17	2	-17	-10.14	Xianggeli	-27	-23	-31	-57	-34.50
Jiangcheng	50	41	16	19	31.60	Xiaojing	-50	-45	-49	-1	-36.25
Jingdong	-8	35	18	10	13.93	Xichang	-44	-52	-55	-69	-55.00
Jiulong	-13	-40	-28	-73	-38.50	Xinlong	-30	-40	-36	-55	-40.25
Kangding	-19	-32	-38	17	-18.00	Yanyuan	-31	-48	-59	-37	-43.75
Kunming	-14	54	12	-78	-6.51	Yuanjiang	-14	4	4	-18	-6.03
Lancang	18	49	17	12	23.97	Yuanmou	18	-34	8	-112	-29.91

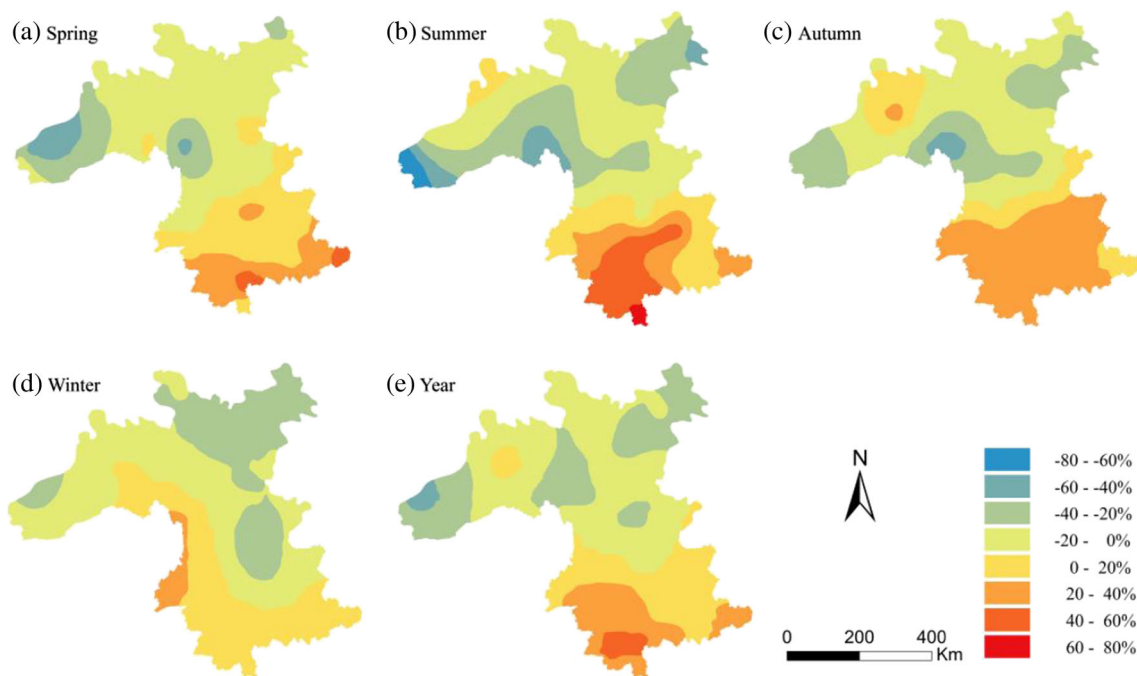


**Fig. 3** Spatial distribution of deviation between TRMM 3B43 precipitation data and meteorological station precipitation data. **a** Spring(March, April, and May). **b** Summer (June, July, and August). **c** Autumn (September, October and November). **d** Winter (December,

January, and February). Data from the deviation of precipitation data from meteorological stations and TRMM 3B43 precipitation data and using spatial interrelation by ARCGIS

the observed data, with the greatest deviation between the northwest, northeast, and three parallel rivers area located in the west of the southwest monsoon region.

### 4 Discussions

#### 4.1 The influence factors of deviation TRMM 3B43 and weather observation data

The deviation between TRMM 3B43 and meteorological observation data showed a positive trend with the increase in altitude (Fig. 4). This was likely due to smaller error in the oceanic and plains regions, which was low in latitude but

greater in high latitude areas such as the mountains and plateaus. Therefore, the meteorological observation data in low altitudes more closely resembled the TRMM data. The TRMM 3B43 precipitation is low in high altitude areas, which was mainly due to the varied topography and dynamic climate of the study area, which, taken together, facilitates the fall of torrential rain. The TRMM data is based on the borne microwave, although it is not fully estimated on underlying surface factors.

#### 4.2 Spatial distribution of annual average precipitation based on TRMM 3B43 data

The annual precipitation in the southwest monsoon region varied between 1000 and 1500 mm and the spatial heterogeneity was significantly different by season (Fig. 5). On the horizontal distribution (Fig. 5), the precipitation in the southern tip of the southwest monsoon region was more similar to the average value at 1197–2100 mm. In the northwest part of the southwest monsoon region, the upper stream of the Yalong River area, north of Mt. Ningjing and Shaluli, the average value of precipitation was less than 1200 mm. During the spring (Fig. 5a), precipitation was scarce throughout the southwest monsoon region. The average precipitation in the northern and central parts was less than 100 mm and less than 400 mm in all other areas. The spatial distribution of precipitation became complex during the summer (Fig. 5b), during which precipitation generally increased to 300 mm or more,

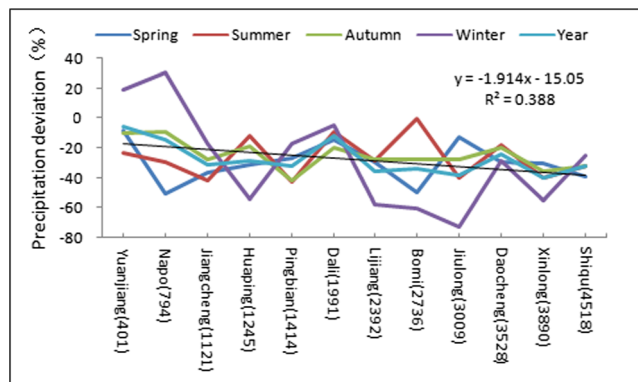


**Fig. 4** The precipitation deviation between TRMM 3B43 data and meteorological station precipitation data at different altitudes

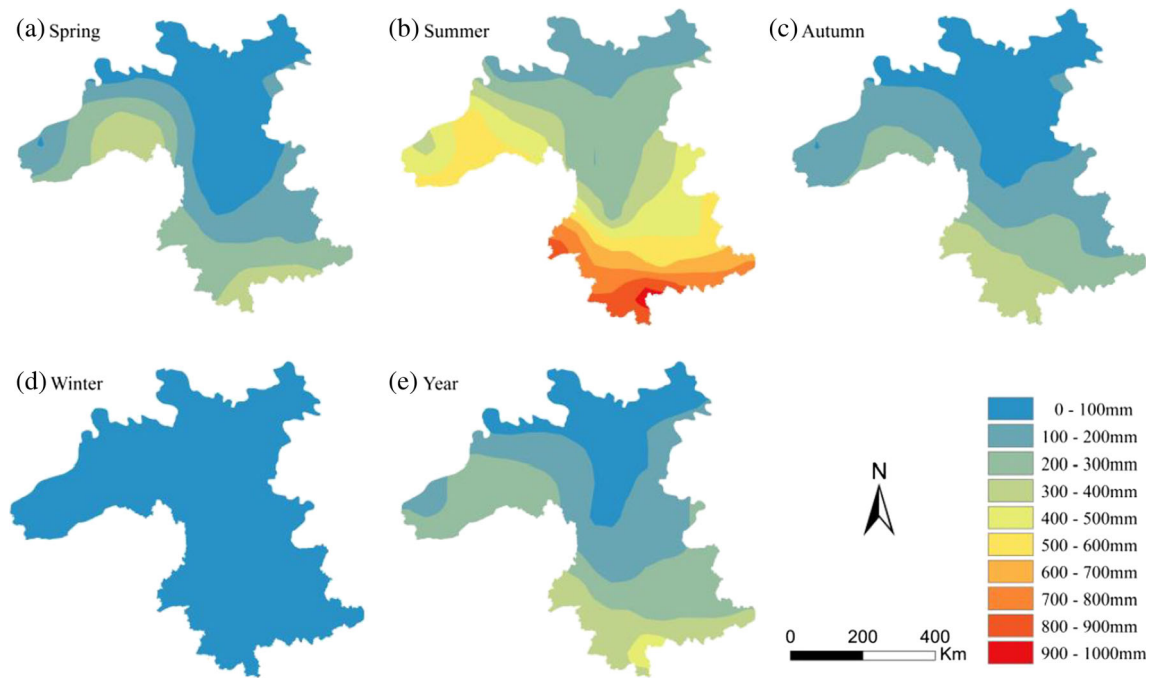


**Fig. 5** Spatial distribution of precipitation based on TRMM 3B43 data in the southwest China monsoon region. **a** Spring (March, April, and May). **b** Summer (June, July, and August). **c** Autumn (September, October and

November). **d** Winter (December, January, and February). Results from precipitation data from 46 meteorological stations using spatial interrelation by ARCGIS

with the spatial distribution being discontinuous from north to south. In theory, the distribution of mountainous terrain would influence the distribution of precipitation. Precipitation was less than 700 mm in the north of the Hengduan Mountains, which was low. The average precipitation in the northwest was less than 300 mm, while in the east of Mt. Shaluli, Haba, and Yun area, the precipitation was greater than 500 mm. There was abundant precipitation in the south, ranging from 700 to 1200 mm. In autumn (Fig. 5c), the weak monsoon weather led to less rainfall, and the low value area expanded to the northwest, Yalong River Basin, and Mt. Jinping. The precipitation was less than 400 mm in the entire southwest monsoon region. There was little precipitation during winter (Fig. 5d), and the precipitation in most areas was generally less than 100 mm in the southwest monsoon region (Fig. 5e). Overall (Fig. 5), the differences in spatial distribution of precipitation were relatively low during the summer and winter. Because the spatial distribution of precipitation was strongly consistent with the atmospheric circulation, atmospheric circulation was similarly stable during summer and in winter. Under the influence of the southwest and southeast monsoon, precipitation was equivalent and spread relatively evenly during the summer. The precipitation was less during the winter, under the influence of the northeastern monsoon, westerlies, and the plateau monsoon. The spatial distribution of precipitation during the spring and winter was similar as it was in the north, where there was a low level of precipitation. However, under the influence of the southwest and southeast monsoon, the spatial distribution of the precipitation high

equivalence region existed in the south of the southwest monsoon region.

### 4.3 Inter-annual variation of precipitation

Precipitation showed a decreasing trend between 1998 and 2011. The tendency rate in spring, summer, autumn, and winter was  $-2.044$ ,  $-10.32$ ,  $-11.074$ ,  $-2.410$ , and  $-0.287$   $\text{mm a}^{-1}$ , respectively. During the spring (Fig. 6a), the precipitation data was obviously fluctuant, with areas in the southwest monsoon region receiving less rainfall except during the years 1998, 2000, 2004, and 2005. The precipitation fluctuation was distinct and showed a decreasing trend in 1998–2011. The most precipitation occurred during the summer of 1999 and the lowest value was in the winter of 2005. Summer precipitation data showed an obvious decreasing trend over the years 1998–2011 (Fig. 6b). During autumn (Fig. 6c), the precipitation tendency trended downward from the northeast to southwest. The precipitation was more fluctuant in summer but decreased during 1998–2001, 2002–2005, and 2006–2008, and increasing during 2002, 2006, and 2009. Compared with other seasons (Fig. 6d), the precipitation value during winter was lower and showed an obvious increasing tendency. In addition, significant variations were present within a single rainfall event. Precipitation was plentiful during 1999 and 2007 but relatively stable in other years. Annually, precipitation showed a decreasing trend, which was similar during summer and autumn (Fig. 6e).

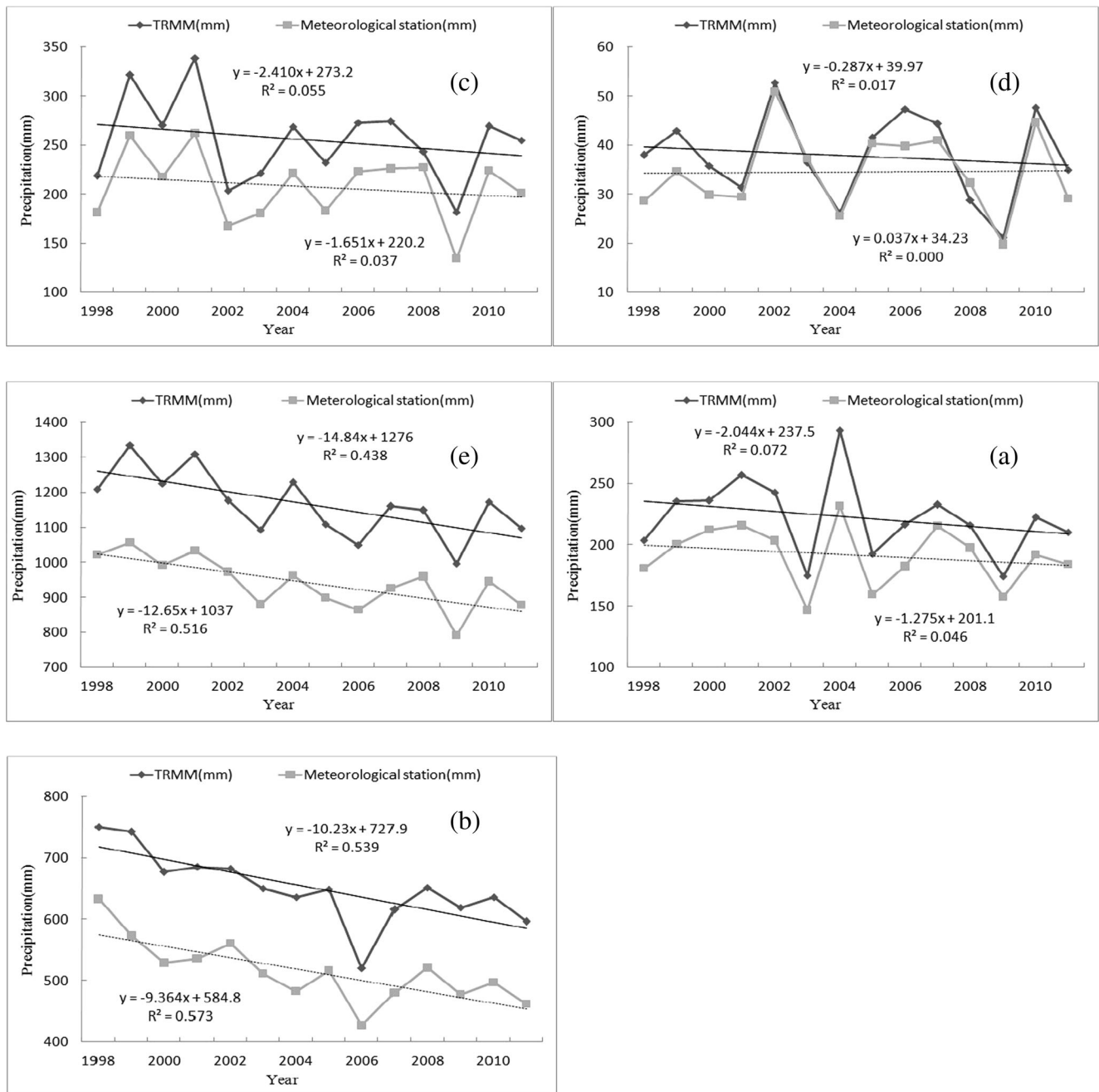


**Fig. 6** Annual variation in precipitation in the southwest China monsoon region. *Black line*: TRMM precipitation data. *Gray line*: meteorological station precipitation data. **a** Spring(March, April, and May). **b** Summer

(June, July, and August). **c** Autumn (September, October and November). **d** Winter (December, January, and February)

### 5 Conclusions

1. The precipitation data obtained by meteorological observation stations was strongly correlated with TRMM 3B43. The TRMM 3B43 data was lower than the observation data. The deviation during spring, summer, autumn, and winter was  $-21.7$ ,  $-22.2$ ,  $-20.4$ , and  $-27.1$  %, respectively.

2. The deviation of TRMM 3B43 and observation data of meteorological stations was greater than 35 % in the northwest, northeast, and southwest of the study area and smaller in the other areas.

3. The spatial distribution of deviation between TRMM 3B43 and meteorological data was differed by season but distributed along the longitudinal mountains in the north and along the southern latitude of the study region.



4. The deviation between TRMM 3B43 and meteorological observation data showed an increasing trend with rise in altitude, and the TRMM 3B43 precipitation data underestimated precipitation at higher altitudes.

**Acknowledgments** This research was funded by the Chinese Postdoctoral Science Foundation (No. 2015M570864), Open-ended Fund of State Key Laboratory of Cryosphere Sciences, Chinese Academy of Sciences (No. SKLCS-OP-2014-11), Northwest Normal University Young Teachers Scientific Research Ability Promotion Plan (No. NWNLU-LKQN-13-10), National Natural Science Foundation of China (No. 41273010, 41271133, 41361106, 41261104), and Major National Research Projects of China (No. 2013CBA01808). We gratefully acknowledge the NASA for the provision of the TRMM data (<http://www.nasa.gov/topics/earth>) and China Meteorological Bureau National Climatic Data Center for provision of the meteorological stations' observation data (<http://www.nmic.gov.cn/>).

## References

- Abbott MB, Bathurst JC, Cunge JA, O'Connell PE, Rasmussen J (1986) An introduction to the European hydrological system—systeme hydrologique European, "SHE", 2: structure of a physically-based distributed modeling system. *J Hydrol* 87(1-2): 61–77. doi:10.1016/0022-1694(86)90115-0
- Awaka, J., Iguchi, T., Okamoto, K., 1998. Early results on rain type classification by the Tropical Rainfall Measuring Mission (TRMM) precipitation radar. Proc 8th URSI Commission F Open Symp, Aveiro, Portugal, 143–146.
- Baguis P, Roulin E, Willems P, Ntegeka V (2010) Climate change scenarios for precipitation and potential evapotranspiration over central Belgium. *Theor Appl Climatol* 99(3-4):273–286. doi:10.1007/s00704-009-0146-5
- Bárdossy A, Lehmann W (1998) Spatial distribution of soil moisture in a small catchment. Part I: geostatistical analysis. *J Hydrol* 206:1–5
- Crave A, Gascuel-odux C (1997) The influence of topography on the time and space distribution of soil surface water content. *Hydrol Process* 11:203–210
- Dinku T, Ceccato P, Grover-Kopec E, Lemma M, Connor SJ, Ropelewski CF (2007) Validation of satellite rainfall products over East Africa's complex topography. *Int J Remote Sens* 28:1503–1526
- Fu YF, Liu GS (2003) Precipitation characteristics in mid-latitude East Asia as observed by TRMM PR and TMI. *J Meteorol Soc Jpn* 81: 1353–1369. doi:10.2151/jmsj.81.1353
- Goovaerts P (1997) *Geostatistics for natural resources evaluation*. Oxford University Press, New York
- Iguchi T, Kozu T, Meneghini R, Awaka J, Okamoto K (2000) Rain-profiling algorithm for the TRMM precipitation radar. *J Appl Meteorol* 39:2038–2052
- Islam MN, Uyeda H (2007) Use of TRMM in determining the climatic characteristics of rainfall over Bangladesh. *Remote Sens Environ* 108:264–276
- Javanmard S, Yatagai A, Nodzu MI, BodaghJamali J, Kawamoto H (2010) Comparing high-resolution gridded precipitation data with satellite rainfall estimates of TRMM\_3B42 over Iran. *Adv Geosci* 25:119–125
- Krajewski WF, Ciach GJ, Habib E (2003) An analysis of small-scale rainfall variability in different climatic regimes. *Hydrological Sciences. J Des Sci Hydrol* 48:151–162.
- Kummerow CD, Barnes W, Kozu T (1998a) The tropical rainfall measuring mission (TRMM) sensor package. *J Atmos Ocean Technol* 15:809–817. doi:10.1175/1520-0426
- Kummerow CD, Barnes W, Kozu T, Shiue J, Simpson J (1998b) The Tropical Rainfall Measuring Mission (TRMM) sensor package. *J Atmos Ocean Technol* 15:808–816. doi:10.1175/1520-0426
- Li, J.J., Su, Z., 1996. *Glacier of Mt. Hengduang*. Science press, Beijing.
- Li L, Hong Y, Wang JH, Adler RF, Policelli FS, Habib S (2009) Evaluation of the real-time TRMM-based multi-satellite precipitation analysis for an operational flood prediction system in Nzoia Basin, Lake Victoria, Africa. *Nat Hazards* 50:109–123
- Li XH, Zhang Q, Xu CY (2012) Suitability of the TRMM satellite rainfalls in driving a distributed hydrological model for water balance computations in Xinjiang catchment, Poyang lake basin. *J Hydrol* 426:28–38
- Liu JF, Chen RS, Han CT (2010) Evaluating TRMM multi-satellite precipitation analysis using gauges precipitation and MODIS snow-cover products. *Adv Water Sci* 21(3):343–348
- Liu Q, Fu YF (2007) Precipitation studies based on TRMM/TMI in Asia. *Sci China Series D* 37(1):111–122
- Liu JF, Chen RS, Qin WW, Yang Y (2011) Study on the vertical distribution of precipitation in mountainous region using TRMM data. *Adv Water Sci* 22(4):447–454
- Nyberg L (1996) Spatial variability of soil water content in the covered catchment of Gardsjon, Sweden. *Hydrol Process* 10:89–103
- Olson WS, Kummerow CD, Heymsfield GM, Giglio L (1996) A method for combined passive-active microwave retrievals of cloud and precipitation profiles. *J Appl Meteorol* 35:1763–1789. doi:10.1175/1520-0450
- Simpson J, Adler RF, North GR (1988) A proposed Tropical Rainfall Measuring Mission (TRMM) Satellite. *Bull Am Meteorol Soc* 69: 278–295
- Schumacher C, Houze RA (2006) Strati form precipitation production over sub-Saharan Africa and the tropical East Atlantic as observed by TRMM. *Q J R Meteorol Soc* 132:2235–2255. doi:10.1256/qj.05.121
- Su FG, Hong Y, Lettenmaier DP (2008) Evaluation of TRMM multisatellite precipitation analysis (TMPA) and its utility in hydrologic prediction in La Plata Basin. *J Hydrometeorol* 9(4):622–640. doi:10.1175/JHM560.1
- Swenson S, Wahr J (2009) Monitoring the water balance of Lake Victoria, East Africa, from space. *J Hydrol* 370:163–176
- Vrieling A, Sterk G, de Jong SM (2010) Satellite-based estimation of rainfall erosivity for Africa. *J Hydrol* 395:235–241
- Western AW, Blöschl G, Grayson RB (1998) Geostatistical characteristics of soil moisture patterns in the Tarrawarra catchment. *J Hydrol* 205: 20–37
- World Meteorology Organization, 1992. *International Meteorological Vocabulary*. World Meteorology Organization, 182~784.
- Yair A, Raz-Yassif N (2004) Hydrological processes in a small arid catchment: scale effects of rainfall and slope length. *Geomorphology* 61: 155–196. doi:10.1016/j.geomorph.2003.12.003
- Yamamoto MK, Furuzawa FA, Higuchi A, Nakamura K (2008) Comparison of diurnal variations in precipitation systems observed by TRMM PR, TMI, and VIRS. *J Clim* 21:4011–4028. doi:10.1175/2007JCLI2079.1
- Yamamoto JK (2005) Correcting the smooth effect of ordinary Kriging estimates. *Math Geol* 37(11):69–94
- Yamamoto JK (2007) On unbiased back transform of lognormal kriging estimates. *Comput Geosci* 11:219–234. doi:10.1007/s10596-007-9046-x
- You WH, He DM, Duan CC (2005) Climate change of the longitudinal range-gorge in Yunnan and its influence on the river flow. *Acta Geograph Sin* 60(1):95–105
- Yu RC, Yuan WH, Li J, Fu YF (2010) Diurnal phase of late-night against late-afternoon of stratiform and convective precipitation in summer southern contiguous China. *Clim Dyn* 35(4):567–576. doi:10.1007/s00382-009-0568-x

- Zeng HW, Li LJ (2011) Accuracy Validation of TRMM 3B43 Data in LancangRiverBasin. *Acta Geograph Sin* 66(7):994–1004
- Zheng D, Bastiaanssen W,GM (2013) First results from Version 7 TRMM 3B43 precipitation product in combination with a new downscaling–calibration procedure. *Remote Sens Environ* 131:1–13.
- Zhu GF, He YQ, Pu T, Wang XF, Jia WX, Li ZX, Xin HJ (2012) Spatial distribution and temporal trends in potential evapotranspiration over Southwest monsoon region from 1960 to 2009. *J Geogr* 22(1):71–85. doi:[10.1007/s11442-012-0912-7](https://doi.org/10.1007/s11442-012-0912-7)